Multi-Impairment Compensation for CO-OFDM System Based on Deep Learning and LDPC Code

Cong Hu, Yuanxiang Chen, *Member, IEEE*, Ying Han, and Jianguo Yu

***Abstract*—In this article, we propose a multi-impairment compensation scheme based on deep learning and low-density parity-check (LDPC) code for the coherent optical orthogonal frequency division multiplexing (CO-OFDM) system. We first propose a multi-impairment compensation autoencoder (MICAE) based on deep neural network (DNN). Then we combine the proposed MICAE with LDPC code and design a DNN-based decoder for LDPC decoding to replace the traditional belief propagation (BP) decoder. The proposed scheme can compensate for multiple impairments simultaneously and has faster decoding speed, greatly improving the performance of the CO-OFDM transmission system. We demonstrate the superiority of the proposed scheme through simulations in different CO-OFDM transmission systems. Simulation results show that the proposed scheme can effectively improve the Q-factor and reduce the bit error rate (BER) of the system, and is more suitable for complex long-distance and high-speed optical transmission scenarios.**

***Index Terms*—Coherent optical orthogonal frequency division multiplexing (CO-OFDM) system, deep learning, low-density parity-check (LDPC) code, multiple impairments compensation.**

I. Introduction

With the increasing demand for data service, optical fiber communication, as the basic support of communication, is confronted with unprecedented challenges. The effective methods to increase transmission capacity include high order phase modulation and channel multiplexing. However, with the increase of modulation order and channel multiplexing density, the transmission distance of high-speed optical fiber communication system is also limited. Coherent optical orthogonal frequency division multiplexing (CO-OFDM) is considered as a promising scheme for future applications in the field of long-distance optical transmission due to its high spectrum efficiency [1], [2]. In long-distance optical transmission system, the OFDM signal suffers various impairments such as chromatic dispersion, polarization-mode dispersion, fiber nonlinearity and phase noise. Impairment compensation and channel coding are two effective ways to improve performance. The former compensates for impairments, while the latter improves the anti-interference ability of the signal.

To compensate for the impairments, a lot of individual schemes such as nonlinearity compensation and phase noise suppression are proposed in [3], [4], [5]. However, in these traditional schemes, the compensation is limited to specific impairment and some compensation algorithms are relatively complicated. A general compensation algorithm is urgently needed for optical communication system. With the application of deep learning in communication, some research results show that the deep learning can effectively improve the performance of communication systems [6]. Deep learning will become an indispensable tool for the design of future communication network and it can be a complement of traditional techniques [7]. Recently, a deep learning model called autoencoder (AE) has been proposed for wireless, non-coherent optical and visible light communications in [8], [9], [10]. In [11], an end-to-end deep neural network (DNN) with joint optimization is implemented for optical fiber communication systems. A new peak to average power ratio (PAPR) reduction scheme based on joint traditional algorithm and machine learning is introduced in [12].

Channel coding improves the performance of long-distance optical transmission by enhancing the anti-interference ability of the signal. Low-Density Parity-Check (LDPC) code is widely used due to its characteristics of performance close to the Shannon limit, flexible structure, and strong error correction ability. The integration of the impairment compensation and LDPC code will produce unexpected results. In general, the neural network (NN) can effectively explore the relationship between input and output. Some researchers find that the NN can perfectly learn the encoding structure with noiseless codewords as training data [13]. The author in [14] thinks that the training samples with noise limit the learning ability of the NN. For this reason, most schemes are composed of a denoising module and a decoder [15], [16]. Nevertheless, these solutions have not used deep learning-based decoders.

Deep learning can quickly and effectively handle complex non-linear problems. In CO-OFDM systems, it can accurately compensate for multiple impairments and accelerate LDPC decoding speed. Inspired by this, in this article, we propose an effective scheme that combines deep learning and LDPC code to improve the performance of CO-OFDM systems in long-distance and high-speed optical transmission scenarios. Firstly,

Manuscript received 13 December 2023; revised 6 February 2024; accepted 20 February 2024. Date of publication 27 February 2024; date of current version 21 March 2024. This work was supported in part by the National Natural Science Foundation of China under Grant 62271079, Grant 61875239, and Grant 62127802, in part by the Fundamental Research Funds for the Central Universities under Grant 2023PY01, in part by the National Key Research and Development Program of China under Grant 2018YFB2200903, and in part by Beijing Nova Program under Grant Z211100002121138. *(Corresponding author: Yuanxiang Chen.)*

The authors are with the School of Electronic Engineering, Beijing University of Posts and Telecommunications, Beijing 100876, China (e-mail: 1134970320@bupt.edu.cn; chenyxmail@bupt.edu.cn; hany5@chinatelecom.cn; yujg@bupt.edu.cn).

Digital Object Identifier 10.1109/JPHOT.2024.3370191

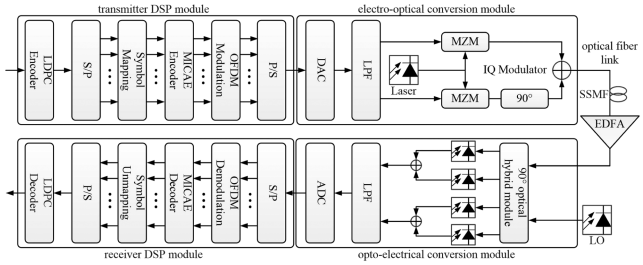

Fig. 1. LDPC-coded CO-OFDM system model.

we propose a multi-impairment compensation autoencoder (MICAE) based on deep learning to capture and compensate impairments suffered in the optical fiber transmission system. The MICAE consists of two DNNs with corresponding structures called encoder and decoder, which are respectively applied to the transmitter and receiver of the transmission system. Through effective data training, the MICAE can flexibly adjust its parameters and accurately capture the impairments in the channel. Then we integrate the proposed multi-impairment compensation scheme and LDPC code in the CO-OFDM system, and design a DNN-based decoder to replace the traditional decoder for LDPC decoding. The proposed decoder can give full play to its low decoding delay characteristics in the long-distance and high-speed transmission scenario. We validate the performance of the proposed scheme in various transmission scenarios. Simulation results show that the proposed scheme has a higher Q-factor and lower bit error rate (BER). Meanwhile, we demonstrate that the combination of the impairment compensation and LDPC code can indeed effectively increase transmission distance.

The rest of the article is organized as follows. The LDPC-coded CO-OFDM system model is described in Section II. Section III provides the technique principle of the proposed scheme. Section IV shows the simulation setup. Simulation results and analyses are discussed in Section V. Section VI concludes the article.

II. System Model

The overall LDPC-coded CO-OFDM system model is shown in Fig. 1, which consists of the transmitter digital signal processing (DSP) module, electro-optical conversion module, optical fiber link, opto-electrical conversion module, and receiver DSP module.

In the transmitter DSP module, the transmitted bit sequence is first LDPC encoded. Then, the LDPC-encoded bit sequence is converted into the parallel complex sequence through serial-parallel conversion and symbol mapping. Furthermore, the real and imaginary parts of the complex sequence are fed into the proposed MICAE. At the output of the MICAE, two predicted real sequences are generated, and a complex sequence is obtained by combining these two real sequences. Finally, the complex sequence performs the OFDM modulation process, including normalization, inserting pilots and guard intervals, and IFFT operation. In the receiver DSP module, corresponding operation is performed to recover the original signal. In addition, we can optionally add the DNN-based LDPC decoder module to accelerate decoding speed. During the training process, the LDPC decoder optimizes its network parameters by continuously reducing the loss. After training, it can be used to decode the bit sequence.

In the electro-optical conversion module, the digital OFDM signal generated by the transmitter DSP module is first converted into an analog signal through a digital-to-analog converter (DAC), and then filtered by a low-pass filter (LPF) and amplified by an amplifier. Furthermore, the amplified in-phase and quadrature components are input together into the IQ modulator consisting of a 90° phase shifter and two Mach-Zehnder modulators (MZM) to achieve orthogonal modulation. Finally, the modulated in-phase and orthogonal components are combined into one optical signal through the coupler. Correspondingly, the opto-electrical conversion module obtains the in-phase and orthogonal components of the signal by performing coherent detection. The optical fiber link is composed of optical fibers and optical amplifiers. In our work, the optical fiber link is segmented, with each segment consisting of 80 km standard single-mode fiber (SSMF) and an erbium-doped fiber amplifier (EDFA).

III. Proposed Scheme

As a typical unsupervised deep learning model, AE can effectively perform feature learning. It usually consists of an encoding network and a decoding network, where the encoding network is used to learn the potential representation of the input data, and the decoding network is used to reconstruct the original data. Assuming the input data is $x = \{x_1, x_2, \ldots, x_N\}$, the feature variable is $z = \{z_1, z_2, \ldots, z_M\}$, and the output data is $\hat{x} = \{\hat{x}_1, \hat{x}_2, \ldots, \hat{x}_N\}$. The output of the L-th layer of the AE encoder is represented as:

$$z^{(l)} = \sigma\left(W_E^{(l)} z^{(l-1)} + b_E^{(l)}\right),\ l = 1, 2, \ldots, L \tag{1}$$

where $N > M$, $W_E^{(l)}$ and $b_E^{(l)}$ represent the weight and bias of the l-th layer, σ is the Sigmoid activation function, $z^{(l)}$ is the feature representation of the l-th layer, and $z^{(0)} = x$. The output of the L-th layer of the AE decoder is represented as:

$$\hat{x}^{(l)} = \sigma\left(W_D^{(l)} \hat{x}^{(l+1)} + b_D^{(l)}\right),\ l = L, L-1, \ldots, 1 \tag{2}$$

where $W_D^{(l)}$ and $b_D^{(l)}$ represent the weight and bias of the l-th layer, $\hat{x}^{(L+1)} = z^{(L)}$ and $\hat{x}^{(1)} = \hat{x}$.

During the training process, the AE first encodes the input data x to obtain the feature variable z, and then decodes z to obtain the output data $\hat{x}$. The purpose of AE is to optimize the network parameters to make the output data $\hat{x}$ as equal as possible to the input data x. Therefore, the objective function of the AE is to minimize the reconstruction error between x and $\hat{x}$, that is,

$$\underset{W_E, W_D, b_E, b_D}{\arg\min}\ L = \sum_{i=1}^{N} ||\hat{x}_i - x_i||_2^2 \tag{3}$$

where $||\cdot||_2$ represents the L2 norm. The above problem can be solved by the stochastic gradient descent method. When the error

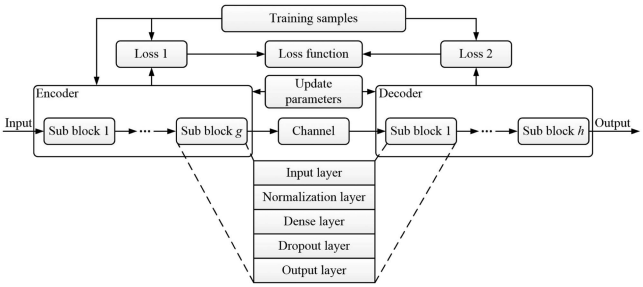

Fig. 2. Network structure and training process of the MICAE.

reaches the minimum value, the optimal network parameters can be obtained.

In our proposed MICAE, the encoder is deployed in the transmitter to preprocess the transmission signal, and the decoder is deployed in the receiver to reconstruct the signal and compensate for the impairment. The network structure and training process of the MICAE is shown in Fig. 2. The encoder and decoder of the MICAE consist of multiple sub blocks, each of which consists of an input layer, a normalization layer, three dense layers, a dropout layer, and an output layer. The normalization layer is used to normalize the input data, which is beneficial for improving the stability and generalization ability of network training. The dense layer contains multiple neurons, and neurons in the same layer are not connected, while neurons in adjacent layers are connected for data transmission. To prevent overfitting, we add a dropout layer before the output layer. Meanwhile, to reduce computational costs and avoid gradient explosion and vanishing problems, we choose ReLU function as the activation function of the dense layer.

In the training process, the parameters of the encoder and decoder are simultaneously adjusted according to the loss function. Different from the traditional AE with loss function of mean square error (MSE), we design a new loss function, which is given as

$$L_{AE} = \lambda L_1(x, \hat{x}) + L_2(x, z) \tag{4}$$

where L_1 is the MSE, which represents the difference between the true value and the predicted value. The additional term L_2, which measures the discrepancy between the input data x and the feature variable z, is introduced to constrain the constellation point spread of the signal. The weighting factor λ allows for fine-tuning the balance between the reconstruction error and the constellation point spread. By adjusting λ, we can prioritize the reconstruction error or the constellation point spread depending on the specific requirements of the task at hand [17]. Through optimization, the value of the λ is determined to be 0.1. The loss function of L_1 and L_2 are calculated as the following equations

$$L_1 = \frac{1}{N}\sum_{i=1}^{N}(x_i - \hat{x}_i)^2 \tag{5}$$

$$L_2 = \frac{1}{N}\sqrt{\sum\nolimits_{i=1}^{N}(x_i - z_i)^2} \tag{6}$$

TABLE I
COMPLEXITY ANALYSIS OF THE MICAE

Layer	Encoder	Decoder
Input Layer	-	-
Normalization Layer	$O(ND)$	$O(ND)$
Dense Layer 1	$O(N(DL+L))$	$O(N(DL+L))$
Dense Layer 2	$O(N(L^2+L))$	$O(N(L^2+L))$
Dense Layer 3	$O(N(L^2+L))$	$O(N(L^2+L))$
Dropout Layer	$O(NL)$	$O(NL)$
Output Layer	$O(N(LD+D))$	$O(N(LD+D))$

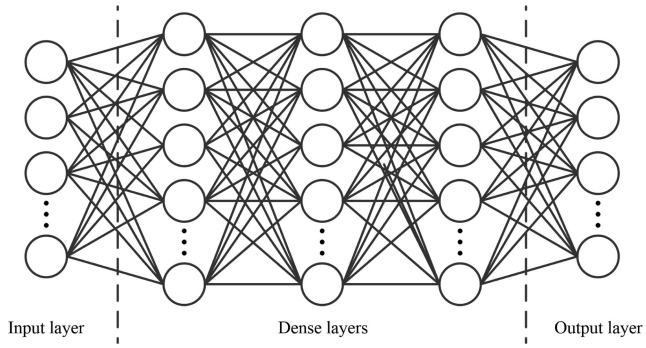

Fig. 3. Structure of the proposed DNN-based LDPC decoder.

where x is the input data, z is the feature variable, and $\hat{x}$ is the output data.

Next, we analyze the complexity of the MICAE. We assume that the length of the input sequence is N, the number of features is D, and the number of neurons in each dense layer is L. The complexity analysis of each layer in MICAE is demonstrated in Table I.

LDPC code is a linear block code based on sparse check matrix, characterized by very few non-zero elements in the check matrix H, which ensures that decoding complexity and minimum code distance only increase linearly with code length. Usually, the LDPC code can be represented by $(n,\ k)$, where n is the total length after encoding, k is the length of information bits, and $m = n - k$ is the length of check bits. Assuming the information bit sequence is b, and the encoded bit sequence is c. The H and c satisfy

$$H \times c^T = 0 \tag{7}$$

The generator matrix G and check matrix H satisfy

$$G \times H^T = 0 \tag{8}$$

Therefore, the c can be obtained by the following formula

$$c = G \times b \tag{9}$$

The most widely used decoding algorithm for LDPC code is the probability-based belief propagation (BP) algorithm. However, since BP algorithm requires constant iterations, when the transmission environment is poor, it will cause a larger transmission delay. Consequently, we design a DNN-based decoder for LDPC code, which consists of an input layer, three dense layers, and a output layer. The structure of the proposed LDPC decoder is shown in Fig. 3. The input and output of the DNN should match the size of matrix H. We explore the relationship between input and output through multiple neurons in the DNN, where

linear relationships are achieved through weights and biases, and nonlinear relationships are implemented through activation functions. After training, the DNN can replace highly complex algorithms, such as channel decoding. We set the loss function to MSE to reduce the error between the predicted value and the true value, represented as follows

$$L_{DNN} = \frac{1}{k}\left(\widehat{b} - b\right)\left(\widehat{b} - b\right)^{T} \tag{10}$$

where T represents the transpose operation, and $\hat{b}$ is the estimated value of the original information b. We respectively use the received information sequence and decoded bit sequence as the input and label of the LDPC decoder, and train the DNN by continuously reducing the loss function L_{DNN} to learn the decoding rule of the LDPC code.

IV. Simulation Setup

In our work, the optical fiber transmission system is realized by VPI Design Suite 9.8. The transmission signal is generated by the DSP module at the transmitter. Different from the traditional CO-OFDM system, we add the MICAE and DNN-based LDPC decoder to the DSP module. Firstly, the electrical signal output from the DSP module is converted into an optical signal. Then the optical signal is sent into the optical fiber which has N spans, each consisting of 80 km SSMF, exhibiting effects of chromatic dispersion, nonlinearity, high birefringence (HIBI), and polarization dependent loss (PDL). To compensate for fiber span loss, each fiber span is connected through an EDFA. This channel model is based on the classical theory of optical fiber communication systems [18], [19]. The combination of SSMF and EDFA simulates the actual fiber optic link as much as possible. Finally, coherent detection is used to recover the optical signal that has suffered channel impairments into an OFDM frames. The DSP module of the receiver will reconstruct the transmission signal.

In the optical fiber transmission system, the linewidth of the transmitting laser and local oscillator (LO) laser is 100 kHz. We set the transmission distance to be between 0 and 560 km, and the transmission rates to be 10 GS/s and 20 GS/s. In the DSP module, the number of OFDM subcarriers is set to 128, the guard interval is 8, zeros is 8, pilots is 10, cyclic prefix is 16, and the size of the check matrix of LDPC code is (16, 32). In MICAE, the settings of the encoder and decoder are consistent. The input and output sizes of the MICAE should match the number of OFDM subcarriers. Considering that the number of subcarriers in the complex OFDM signal is 128, and the input and output of the MICAE are only real numbers, we set the input and output sizes of the MICAE to 256. The activation function of the dense layer is set to ReLU function, which is the most commonly used activation function. We use randomly generated 10240000-bit binary sequence as the training sample. To limit the output of the MICAE to discrete binary numbers, we use Sigmoid function as the activation function of the output layer. In order to reduce the loss value and improve the convergence speed during training, we use the Adam optimizer to optimize the parameters of the network. The number of neurons in dense layer, initial learning rate, and batch size are obtained through optimization, and set to 2048, 0.01, and 512, respectively. The learning rate decreases as training progresses, with a decay factor of 0.5. The detail setting of the proposed MICAE is shown in Table II. The LDPC decoder based on DNN consists of one input layer, three dense layers, and one output layer, and the number of neurons in the three dense layers is set to 1024, 256, and 64, respectively. The activation function of the dense layer is set to ReLU function. To limit the output of the decoder to discrete binary numbers, we use Sigmoid function as the activation function of the output layer. The settings of other hyperparameters in the network are consistent with those of the MICAE. The input of the training sample comes from the impaired LDPC codeword obtained at the receiver, and the output comes from the input of the LDPC encoder at the transmitter.

TABLE II
Detail Setting of the MICAE

Training parameters	value
Encoder input	256
Encoder output	256
Decoder input	256
Decoder output	256
number of neurons in dense layer	2048
Activation function of dense layer	ReLU
Activation function of output layer	Sigmoid
Optimizer	Adam
Initial learning rate	0.01
Decay factor for learning rate	0.5
Batch size	512

V. Simulation Results

In this section, we first assess the effectiveness of the proposed MICAE through constellation diagram, Q-factor, and BER performance. Then, the performance of the DNN-based decoder is evaluated. Finally, the Q-factor and BER performance of the proposed combination scheme are analyzed.

A. Performance of MICAE

We add the encoder and decoder of MICAE to the transmitter and receiver of the CO-OFDM system, respectively. The improved CO-OFDM system can effectively compensate multiple impairments. We transmit the 4QAM-OFDM signal at a transmission rate of 10 GS/s. The constellation diagrams of the CO-OFDM system before and after using the MICAE are shown in Fig. 4. The first row in Fig. 4 represents the constellation diagrams of the traditional uncompensated scheme obtained at the receiver, and the second row represents the constellation diagrams of the proposed compensation scheme obtained at the receiver. The transmission distances are set to 80 km, 160 km, 240 km, 320 km from left to right. It can be clearly seen that the constellation points of the proposed scheme are more concentrated, which means smaller noise. That is, the probability of decision errors and the BER of the proposed scheme are lower.

We use Q-factor to measure the performance of the CO-OFDM system, which represents the ratio of receiver decision level signal to noise. We compare the Q-factor of the proposed MICAE with traditional uncompensated scheme. Fig. 5 shows

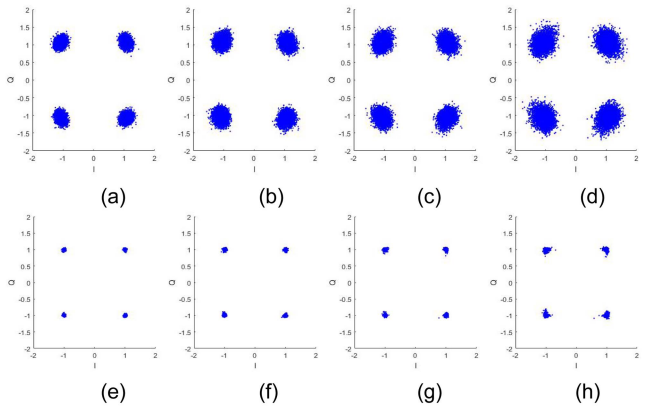

Fig. 4. Constellation diagram of CO-OFDM system before and after using MICAE. (a) Traditional scheme 80 km, (b) traditional scheme 160 km, (c) traditional scheme 240 km, (d) traditional scheme 320 km, (e) proposed scheme 80 km, (f) proposed scheme 160 km, (g) proposed scheme 240 km, and (h) proposed scheme 320 km.

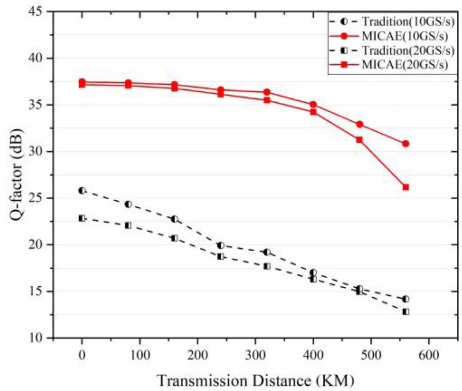

Fig. 5. Q-factor of the CO-OFDM system under different transmission distances and transmission rates.

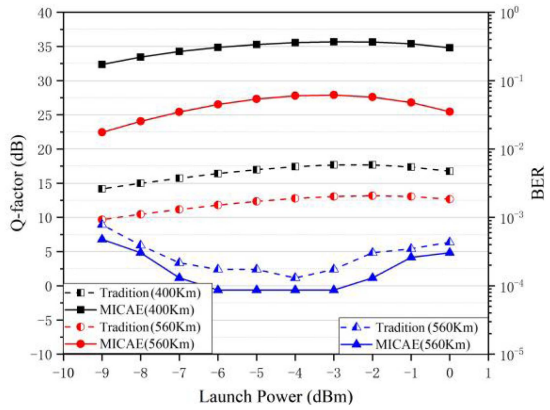

Fig. 6. Performance of the CO-OFDM system under different launch powers.

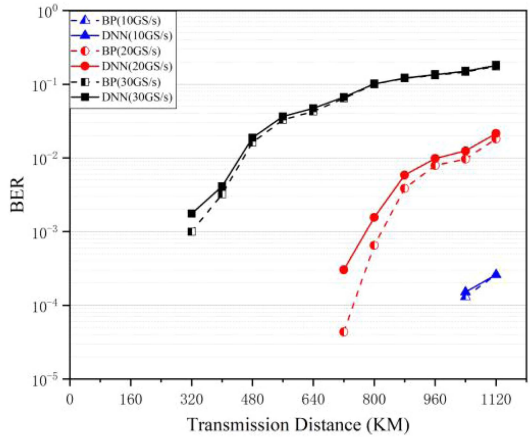

Fig. 7. BER of the LDPC-coded CO-OFDM system with MICAE and DNN decoder.

the performance of various schemes under different transmission distances and transmission rates. We first use 4QAM-OFDM signals with transmission rates of 10 GS/s and 20 GS/s, transmission distances of 0∼560 km, and intervals of 80 km to train the MICAE. Then, we verify the performance of the trained MICAE under different transmission distances and transmission rates. The figure shows that when the transmission rate is fixed and the transmission distance is from 0 to 560 km, the proposed scheme has a Q-factor at least 10 dB higher than the traditional scheme. This indicates that the MICAE can achieve excellent performance within the training sample range. This provides a foundation for exploring the robustness of MICAE under broader conditions.

Fig. 6 indicates the performance of the proposed scheme under different launch powers. We transmit the 4QAM-OFDM signal at a transmission rate of 20 GS/s. We set the transmission distance to 400 km and 560 km respectively, and gradually adjust the transmission power from 0 to -10 dBm. In Fig. 6, the solid line represents the proposed scheme, and the dashed line represents the traditional scheme. The square and circular curves represent the Q-factors of the two methods at transmission distances of 400 and 560 km, respectively, while the triangular curve represents the BER at a transmission distance of 560 km (the BER is 0 at a transmission distance of 400 km). Obviously, our proposed scheme has better performance than the traditional scheme under different launch powers. When the transmission power is -3 dBm, the proposed method has the highest Q-factor and the lowest BER.

B. Performance of DNN-Based Decoder

We introduce LDPC code in the CO-OFDM system and utilize the proposed DNN-based decoder to replace the traditional BP decoder for LDPC decoding. Fig. 7 indicates the BER performance of the LDPC-coded CO-OFDM system with various decoders. As observed from this figure, the BER performance improvement brought by the DNN-based decoder is close to the BP decoder. However, with the increase of the transmission distance and transmission rate, the signal will suffer more serious impairments. Therefore, the BP decoder requires more iterations to achieve excellent performance, leading to an increase in decoding time and transmission delay. For the DNN-based decoder, once the network is trained, its parameters will not change, and the decoding time cost is lower than the BP decoder. Hence, in the long-distance and high-speed optical transmission

scenario, using a DNN-based decoder instead of a BP decoder is a better choice.

C. Performance of Combination Scheme

To improve the transmission performance of the CO-OFDM system, we creatively combine the proposed MICAE and LDPC code. Meanwhile, we use the DNN-based decoder to replace the BP decoder. Next, we will use the 4QAM-OFDM signal to evaluate the performance of this combination scheme.

To begin with, we assess the performance of the combination scheme under different transmission distances and transmission rates. We add the proposed MICAE and DNN-based decoder to the DSP module of the LDPC-coded CO-OFDM transmission system. The former is used to compensate for various impairments, and the latter is used to improve the anti-interference ability of the transmission signal. We first use 4QAM-OFDM signals with transmission rates of 10 GS/s, 20 GS/s and 30 GS/s, transmission distances of 0∼640 km, and intervals of 80 km to train the MICAE. Then, we verify the performance of the trained MICAE under transmission distances within 1120 km and transmission rates of 10 GS/s, 20 GS/s and 30 GS/s. Fig. 8 shows the performance of the LDPC-coded CO-OFDM system under different transmission distances and transmission rates. In this figure, the solid line represents the Q-factor and BER performance of the LDPC-coded CO-OFDM system after MICAE is added, and the dashed line represents the performance of the system before MICAE is added. As shown in Fig. 8(a), the Q-factor of the proposed combination scheme has been improved within a transmission distance of 1120 km. However, as the transmission distance increases, the improved performance of the proposed scheme decreases. From Fig. 8(b), it can be seen that when the transmission distance is low, the MICAE indeed helps to improve the BER performance of the system. Similar to Fig. 8(a), as the transmission distance increases, the improved performance decreases. This is because the training samples used by the MICAE come from low transmission distance and we believe that when training the MICAE with samples with high transmission distance and transmission rate, its performance will be improved. Moreover, once the MICAE is trained, its parameters will not change. In practical applications, it only performs forward propagation, thus offering the advantage of lower cost.

In addition, we set the transmission distance to 720 km and 880 km, the transmission rate to 20 GS/s, and measure the transmission performance of the system by continuously adjusting the transmission power. The Q-factor and BER of the LDPC-coded CO-OFDM system under different launch powers are shown in Fig. 9. In this figure, the curves with square and circular points represent the Q-factors of different schemes at transmission distances of 720 km and 880 km, respectively, corresponding to the scale on the left. The curve with triangular points represents the BER of different schemes at a transmission distance of 880 km, corresponding to the scale on the right. It is obvious that the scheme we proposed has greatly improved the transmission performance of the system. Under current

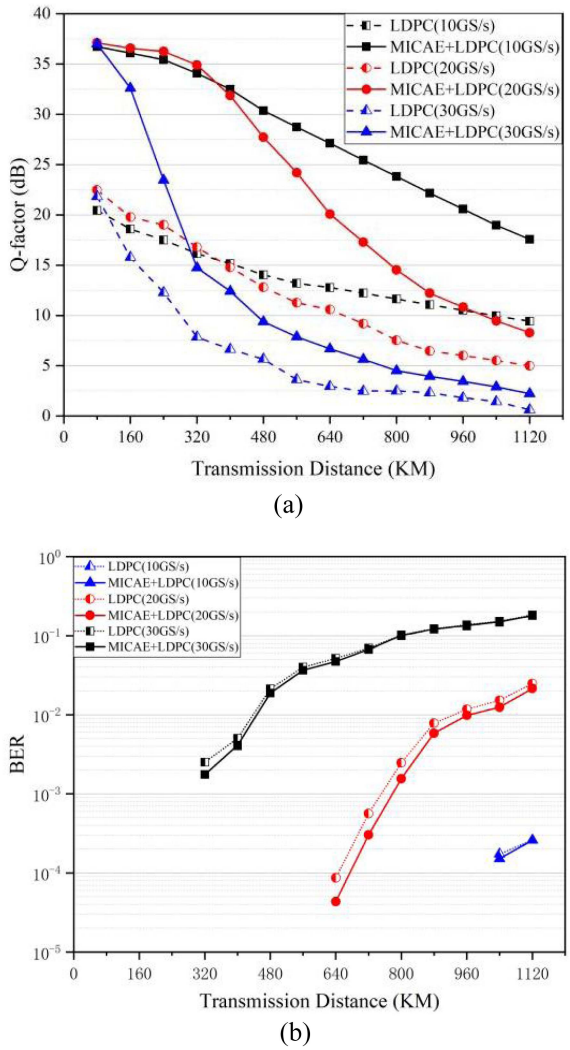

Fig. 8. Performance of the LDPC-coded CO-OFDM system under different transmission distances and transmission rates. (a) Q-factor. (b) BER.

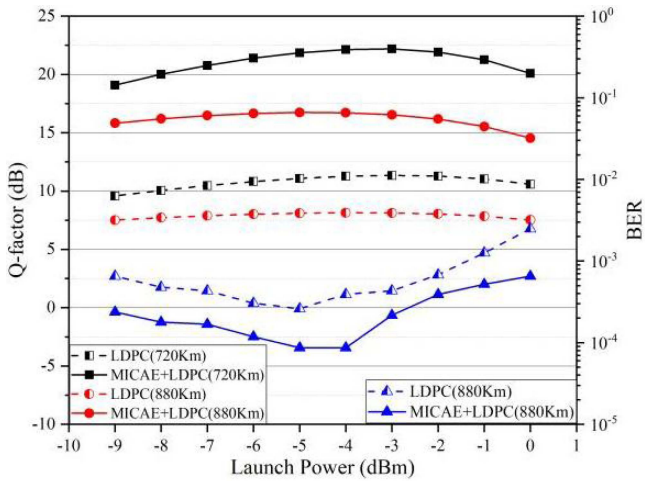

Fig. 9. Performance of the LDPC-coded CO-OFDM system under different launch powers.

transmission conditions, the Q-factor improvement brought by MICAE is about 10 dB. In addition, we should note that the 0 BER performance is achieved at 720 km. Compared with the simulation setup in Fig. 6, the transmission distance has increased by 320 km. In summary, the transmission performance of the proposed combination scheme is undoubtedly superior.

VI. Conclusion

In this article, we proposed a multi-impairment compensation scheme for CO-OFDM system that combines deep learning and LDPC code. We first developed a MICAE to compensate for impairments suffered in optical fiber communication system. Then, to fully leverage the advantages of the MICAE and LDPC code, we combined them and designed a DNN-based decoder for LDPC decoding. We verified the superiority of the proposed scheme through simulations in different transmission scenarios. Simulation results show that the proposed scheme has better performance and is suitable for the complex long-distance and high-speed optical transmission scenario.

References

[1] L. Liu et al., "High performance and cost effective CO-OFDM system aided by polar code," *Opt. Exp.*, vol. 25, pp. 2763–2770, 2017.

[2] X. Tang et al., "A physical layer security-enhanced scheme in CO-OFDM system based on CIJS encryption and 3D-LSCM chaos," *J. Lightw. Technol.*, vol. 40, no. 12, pp. 3567–3575, Jun. 2022.

[3] E. Giacoumidis, A. Tsokanos, M. Ghanbarisabagh, S. Mhatli, and L. P. Barry, "Unsupervised support vector machines for nonlinear blind equalization in CO-OFDM," *IEEE Photon. Technol. Lett.*, vol. 30, no. 12, pp. 1091–1094, Jun. 2018.

[4] L. N. Venkatasubramani, A. Vijay, D. Venkitesh, and R. D. Koilpillai, "Pilot-free common phase error estimation for CO-OFDM with improved spectral efficiency," *IEEE Photon. J.*, vol. 11, no. 6, Dec. 2019, Art. no. 7205210.

[5] Y. Xu, X. Du, S. Liu, and C. Yu, "Number-theoretic net-based particle filtering for linear phase noise tracking in CO-OFDM systems," in *Proc. 20th Int. Conf. Opt. Commun. Netw.*, 2022, pp. 1–3.

[6] C. Hu et al., "Digital self-interference cancellation for full-duplex systems based on deep learning," *AEU-Int. J. Electron. Commun.*, vol. 168, 2023, Art. no. 154707.

[7] A. Jagannath, J. Jagannath, and T. Melodia, "Redefining wireless communication for 6G: Signal processing meets deep learning with deep unfolding," *IEEE Trans. Artif. Intell.*, vol. 2, no. 6, pp. 528–536, Dec. 2021.

[8] Z. Huang, D. He, J. Chen, Z. Wang, and S. Chen, "Autoencoder with fitting network for terahertz wireless communications: A deep learning approach," *China Commun.*, vol. 19, no. 3, pp. 172–180, Mar. 2022.

[9] C. Zou, F. Yang, J. Song, and Z. Han, "Wideband underwater wireless optical communication based on multi-carrier autoencoder," *IEEE Wireless Commun. Lett.*, vol. 10, no. 11, pp. 2494–2498, Nov. 2021.

[10] A. Mohamed, A. S. T. Eldien, M. M. Fouda, and R. S. Saad, "LSTM-autoencoder deep learning technique for PAPR reduction in visible light communication," *IEEE Access*, vol. 10, pp. 113028–113034, 2022.

[11] B. Karanov et al., "End-to-end deep learning of optical fiber communications," *J. Lightw. Technol.*, vol. 36, no. 20, pp. 4843–4855, Oct. 2018.

[12] T. Zhang, Z. Tong, W. Zhang, H. Wang, and P. Li, "A novel PAPR reduction scheme based on joint traditional algorithm and machine learning for CO-OFDM systems," *IEEE Photon. Technol. Lett.*, vol. 35, no. 8, pp. 418–421, Apr. 2023.

[13] W. Lyu, Z. Zhang, C. Jiao, K. Qin, and H. Zhang, "Performance evaluation of channel decoding with deep neural networks," in *Proc. IEEE Int. Conf. Commun.*, 2018, pp. 1–6.

[14] T. Koike-Akino, Y. Wang, D. S. Millar, K. Kojima, and K. Parsons, "Neural turbo equalization: Deep learning for fiber-optic nonlinearity compensation," *J. Lightw. Technol.*, vol. 38, no. 11, pp. 3059–3066, Jun. 2020.

[15] W. Cao, J. He, and Z. Zhou, "Enhanced LDPC based differential iteration decoding scheme for PDM 16-QAM coherent optical communication systems," in *Proc. Conf. Lasers Electro-Opt. Pacific Rim*, 2018, pp. 1–2.

[16] Y. He, M. Jiang, X. Ling, and C. Zhao, "Robust BICM design for the LDPC coded DCO-OFDM: A deep learning approach," *IEEE Trans. Commun.*, vol. 68, no. 2, pp. 713–727, Feb. 2020.

[17] M. Kim, W. Lee, and D.-H. Cho, "A novel PAPR reduction scheme for OFDM system based on deep learning," *IEEE Commun. Lett.*, vol. 22, no. 3, pp. 510–513, Mar. 2018.

[18] G. P. Agrawal, *Nonlinear Fiber Optics*. Cambridge, Massachusetts, USA: Academic, 1995.

[19] W. Shieh, H. Bao, and Y. Tang, "Coherent optical OFDM: Theory and design," *Opt. Exp.*, vol. 16, no. 2, pp. 841–859, 2008.